

Fission probes of sub-barrier fusion cross section enhancements and spin distribution broadening

T. Murakami, C.-C. Sahn, R. Vandenbosch,* D. D. Leach, A. Ray, and M. J. Murphy†

Nuclear Physics Laboratory, University of Washington, Seattle, Washington 98195

(Received 10 March 1986)

The mean-square spin value of the compound nucleus ^{248}Cf has been determined from fission fragment angular distributions for the $^{12}\text{C} + ^{236}\text{U}$ and $^{16}\text{O} + ^{232}\text{Th}$ reactions at sub-barrier bombarding energies. The anisotropy and hence the mean-square spin values are much larger than predicted by models which reproduce the cross section enhancement observed in the sub-barrier fusion excitation functions. A similar experiment with the spherical target ^{208}Pb also leads to larger anisotropies and mean-square spin values than predicted by various fusion models, including an especially complete coupled channels calculation. Supplementary fragment-fragment coincidence experiments have been performed with the heavier targets to confirm that the observed fission is associated with full momentum transfer. The mass distribution for the $^{12}\text{C} + ^{236}\text{U}$ reaction has been measured at two angles and found to be independent of angle. This last result suggests that quasifission processes are not playing a significant role.

I. INTRODUCTION

There has been a renewed interest in sub-barrier fusion with the observation that the cross sections were often larger than initially expected and depend in an interesting way on the nuclear structure of the reacting species.¹⁻⁵ The substantial enhancements of sub-barrier fusion cross sections are usually explained by permanent deformation and by slow shape fluctuations of the nuclei involved. Different orientations between reaction partners with static deformations and the excitation of vibrational modes in the early stage of the reaction lead to different effective fusion barriers and hence to a less steep decrease of the fusion cross section at sub-barrier energies. The same mechanisms, of course, give rise to different impact parameters finally leading to fusion, and thus, the spin distribution of the compound nucleus will be affected as well. The models used to describe the fusion cross section as a function of energy must also explain the compound nucleus spin distribution. Less information has been obtained on the spin distributions in sub-barrier fusion, but near-barrier studies⁶⁻⁹ have showed the broadening of the spin distributions expected from barrier penetration, zero point motion, and permanent deformation.

γ -ray multiplicity techniques have been employed previously in studies of spin distributions in near-barrier fusion.⁶⁻⁹ In such studies fusion events are selected by triggering on a discrete γ transition in a particular evaporation residue. This is most easily done if the residue is a deformed even-even nucleus, in which case almost all of the deexcitation strength ends up in the ground state rotational band. The mean spin of the compound nuclear spin distribution can be determined from the average γ ray multiplicity. This approach was used previously in this laboratory,^{6,7} to study near-barrier fusion of ^{12}C and ^{16}O with the deformed target nucleus ^{154}Sm . It was found that one had to take into account the barrier fluctuations associated with the large deformation of the target to

reproduce the mean spin values. Haas *et al.*⁸ have used the same experimental approach to study the mean-spin value in near-barrier reactions involving vibrational nuclei and concluded that the effects of zero-point vibrations had to be included to account for the mean spin values observed. Nolan *et al.*⁹ have used a potentially more powerful technique involving a multielement array from which the multiplicity distribution can be obtained. They studied one of the systems studied by Haas *et al.*, $^{80}\text{Se} + ^{80}\text{Se}$, to much lower energies, and concluded that the spin distribution extended to higher values than expected for a single one-dimensional barrier. The absolute values of the fusion cross section were not determined, however. Dasso *et al.*¹⁰ have shown that the excitation of vibrational modes can account for the general features of the multiplicity distributions reported by Nolan *et al.*

We report here a new study of the mean-square value of the spin distribution, exploiting the sensitivity of fission fragment angular distributions to the compound nuclear spin distribution. This technique has high sensitivity and can be extended to quite low sub-barrier energies. We have used this approach to study the spin distribution for two entrance channels involving deformed nuclei and leading to the compound nucleus ^{248}Cf . We have also studied the $^{16}\text{O} + ^{208}\text{Pb}$ system where the target nucleus is spherical.

We approached the present study with the expectation that our present understanding of sub-barrier fusion would provide an adequate framework for interpreting our results. This has turned out not to be the case. As reported in a recent paper,¹¹ we have found considerably higher mean-square spin values than expected at sub-barrier energies. We therefore will present our results and their analysis in some detail, paying particular attention to the assumptions made in the analysis and to the constraints imposed in the comparison with model calculations due to the availability of both spin distribution and total fusion cross section data.

II. EXPERIMENT

The experiments were performed using 60–68 MeV ^{16}O and 77–86 MeV ^{16}O beams from the University of Washington Nuclear Physics Laboratory FN Tandem Van de Graaff generator. The beam size was defined by a 0.32 cm diam aperture. Beam currents were 20–300 e nA and targets were typically several hundred $\mu\text{g}/\text{cm}^2$ thick. The isotopic purity of the ^{208}Pb , ^{232}Th , and ^{236}U targets was better than 99%. An array of surface barrier detectors of 5–20 μm thickness was used to detect the fission fragments. For these thicknesses elastically and inelastically scattered oxygen or carbon ions deposit only a fraction of their energy in the detector, permitting unambiguous identification of fission fragments. In some runs the surface barrier detectors were supplemented by a gas ionization counter. The detector array spanned a laboratory angle range between 85° and 170° . The solid angle subtended by each detector was about 6 msr. The geometrical solid angles were verified by calibration with a ^{252}Cf spontaneous fission source. The absolute fission cross sections were determined by normalization to Rutherford scattering using a monitor counter at forward angles.

We measured the fission fragment mass distribution for the reaction $^{238}\text{U}(^{16}\text{O},\text{f})$ at 66 MeV in a separate experiment. The fragment mass was determined using a time-of-flight (TOF) telescope consisting of a channel plate time-zero detector with a 20 $\mu\text{g}/\text{cm}^2$ carbon foil and an array of four 450 mm² surface barrier detectors (SBD's), each 150 μm thick. The flight path was 561 mm; the solid angle covered by the telescope was 5.2 msr. Energy and TOF signals were recorded event by event for each detector separately. The telescope was calibrated using the elastically scattered projectiles and a 5 μCi ^{252}Cf fission source. The pulse-height defect of the SBD's was corrected using the procedure proposed by Kaufman *et al.*¹² In addition, a slightly mass and energy dependent delay time of the fast SBD signal with respect to signals from the ^{12}C projectiles had to be used for fission fragments to reproduce the known Cf fission-fragment mass distribution.

III. RESULTS

A. Angular distributions

The differential cross sections were transformed to the c.m. system assuming full momentum transfer and an average kinetic energy release consistent with the Viola systematics.¹³ The angular distributions for the $^{12}\text{C} + ^{236}\text{U}$ and $^{16}\text{O} + ^{236}\text{U}$ systems have been reported in our earlier paper.¹¹ It was shown that these distributions exhibit about twice the expected anisotropy. The angular distributions obtained for the $^{16}\text{O} + ^{208}\text{Pb}$ reaction are shown in Fig. 1. At 80 MeV our measurements overlap the earlier, in general higher energy, measurements of Videbaek *et al.*¹⁴ Our results are consistent with this earlier measurement. During the course of our measurements, we became aware of a similar study by Vulgaris *et al.*¹⁵ Their distribution at 78 MeV is in good agreement with our distribution at 77.3 MeV. Except for the lowest bombarding energy, these distributions are also more an-

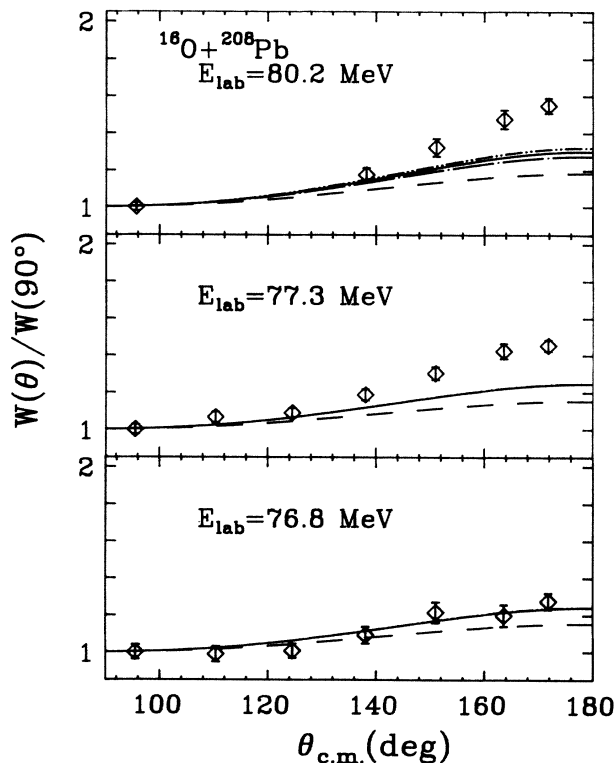


FIG. 1. Angular distribution for the $^{16}\text{O} + ^{208}\text{Pb}$ reaction at three bombarding energies. The solid, dashed, dotted-dashed, and double-dotted-dashed curves represent calculations on the Esbensen, Wong, Pieper *et al.*, and Udagawa *et al.* models, respectively.

isotropic than expected on the basis of model calculations discussed below.

B. Linear momentum transfer

In view of the surprisingly large values of the anisotropies observed, we have made as many experimental checks of our assumptions as possible. The transformation from the laboratory to the c.m. frame increases the observed anisotropy by almost a factor of 2. Previous studies¹⁶ have shown an appreciable component associated with small momentum transfer at much higher bombarding energies. The fraction of fission following inelastic or transfer processes drops from 20% at 140 MeV to 10% at 110 MeV for the $^{16}\text{O} + ^{238}\text{U}$ reaction. Although it seemed unlikely that fission following inelastic or transfer reactions would be important at our lower energies, we made several checks of the momentum transfer by measuring the folding angle between coincident fragments. The results, illustrated in Fig. 2, are consistent with, at most, a few percent contribution of small momentum transfer events. This result is not surprising in view of the large fission barriers (~ 6 MeV) for ^{232}Th , ^{236}U , and neighboring nuclei. Inelastic and transfer reactions with sufficient inelasticity to lead to sequential fission would be very sub-barrier in the exit channel. (See, however, note added in proof.)

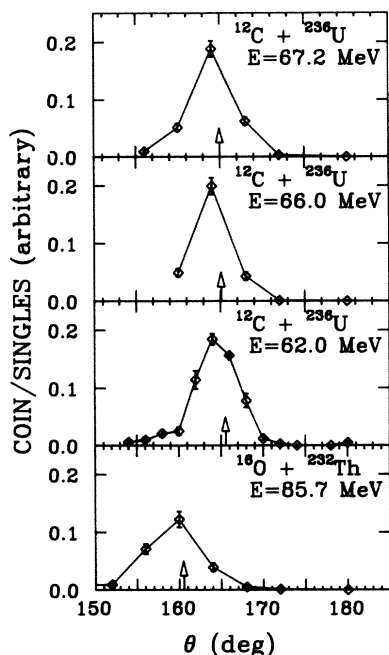


FIG. 2. Coincidence-to-singles ratio as a function of folding angle. The arrow indicates the most probable angle expected for full linear momentum transfer.

C. Excitation functions

In addition to the bombarding energies where we took sufficient data to obtain quantitative angular distribution data, we have also measured the fission yield at other energies with sufficient accuracy to obtain meaningful excitation function data.

The results for the $^{16}\text{O} + ^{208}\text{Pb}$ system are shown in Fig. 3. Also shown are the results of Videbaek *et al.*,¹⁴ Vul-

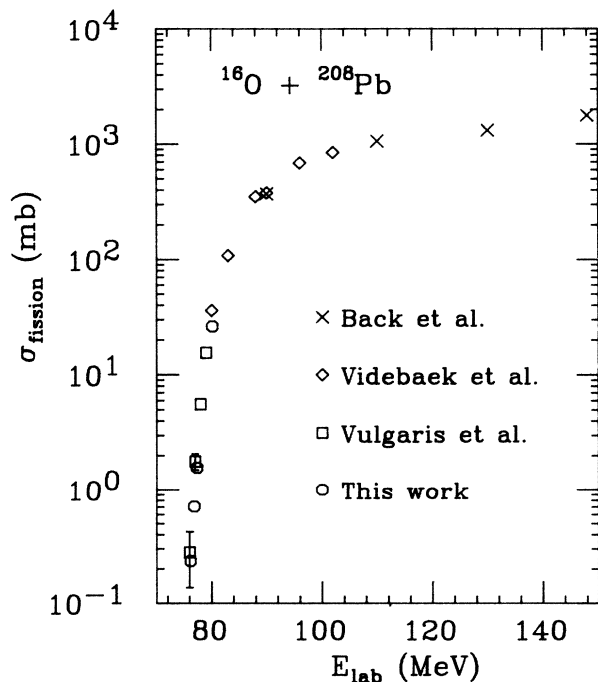


FIG. 3. Fission excitation function for the $^{16}\text{O} + ^{208}\text{Pb}$ reaction.

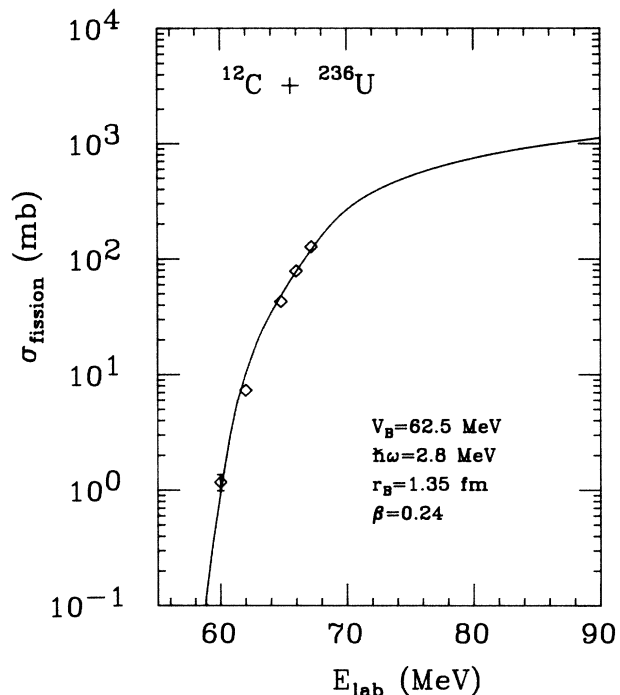


FIG. 4. Fission excitation function for the $^{12}\text{C} + ^{236}\text{U}$ reaction.

garis *et al.*,¹⁵ and Back *et al.*¹⁷ These results all seem to be in reasonable agreement. At low bombarding energy it is necessary to add the evaporation residue cross section to the fission cross section to obtain the total fusion cross section. Vulgaris *et al.* and Hartel¹⁸ have used different approaches to determine the evaporation residue cross section. Vulgaris *et al.* measured the residues directly in a recoil mass spectrometer, whereas Hartel measured the induced α activity. The cross sections of Vulgaris *et al.* are about 3 times smaller than those of Hartel, for reasons

TABLE I. Fission cross sections measured in this work. Errors are statistical; there is an additional error associated with the absolute normalization of approximately 5%.

E_{lab}	σ_{fission}
$^{16}\text{O} + ^{208}\text{Pb}$	
76.2	0.234 ± 0.025
76.8	0.71 ± 0.01
77.3	1.57 ± 0.02
80.2	26.2 ± 0.90
$^{12}\text{C} + ^{236}\text{U}$	
62.0	7.3 ± 0.2
64.8	42.9 ± 1.4
66.0	78.7 ± 1.3
67.2	127.5 ± 2.4
$^{16}\text{O} + ^{232}\text{Th}$	
79.7	4.8 ± 0.6
81.7	12.3 ± 0.9
83.7	26.3 ± 4.9
85.7	63.5 ± 4.9
86.0	76.3 ± 9.5

which are not apparent. We note, however, that the smaller values of Vulgaris *et al.* are reproduced by default parameters of the PACE¹⁹ evaporation code. Since the cause of the discrepancy is not certain, we have averaged the two sets of data to add to the fission cross section to obtain the total fusion cross section for comparison with model calculations. At $E_L=80$ MeV the correction is about 5% and increases to 15% at 76 MeV. The excitation function for the $^{12}\text{C} + ^{236}\text{U}$ system is shown in Fig. 4. The excitation function for the $^{16}\text{O} + ^{232}\text{Th}$ system has been presented in an earlier publication.¹¹ The results of the cross section measurements are summarized in Table I.

D. Mass distributions

The measured mass distributions are shown in Fig. 5. In the top part the Cf calibration spectrum (solid curve) is compared to the mass yield curve taken from the literature.²⁰ From this comparison we conclude that the mass calibration is accurate within approximately 1.5%. The middle and bottom parts show the fission fragment mass distributions from the reaction $^{236}\text{U}(^{12}\text{C},f)$ at 98° and 163° , respectively. The distributions were transformed into the center-of-mass frame under the assumption of full momentum transfer, which was already proven to be justified and by using the measured fragment velocity. The shape of the measured distributions is very much like the shape one would expect from fission of the compound nucleus ^{248}Cf at 38 MeV excitation energy: the distribution is symmetric, as one expects due to the excitation energy, but broad and with an almost flat top due to the underlying asymmetric mass distribution one expects at low and moderate excitation energies. The fission fragment total kinetic energy is not expected to vary much with the excitation energy of the fissioning nucleus. Thus, by using the systematics of the total kinetic energy released in fission¹³ and the neutron binding energy of the most probable fragments,²¹ one can estimate the mean number of neutrons emitted by each fission fragment. With the assumption that the most probable kinetic energy of the neutrons is equal to twice the temperature of the residual nucleus, one finds that, on the average, 4.5 neutrons are emitted from each of the most probable fission fragments. Thus, the first moments of the mass distributions agree well with

TABLE II. Frequencies $\hbar\omega_\lambda$, $B(E\lambda)/B_W$ or β values, and standard deviations σ_λ of low-lying quadrupole and octupole vibrational states.

λ^π		^{208}Pb	^{232}Th	^{236}U
2 ⁺	$\hbar\omega$ (MeV)	4.09	0.049	0.045
	$B(E2)/B_W$	8	$\beta_2=0.22$	$\beta_2=0.24$
	or β_2			
	σ_2	0.11	0.458	0.502
3 ⁻	$\hbar\omega$	2.61	0.77	0.74
	$B(E3)/B_W$	40	29	30
	σ_3	0.243	0.195	0.194
ΔR		0.4	0.6	0.5

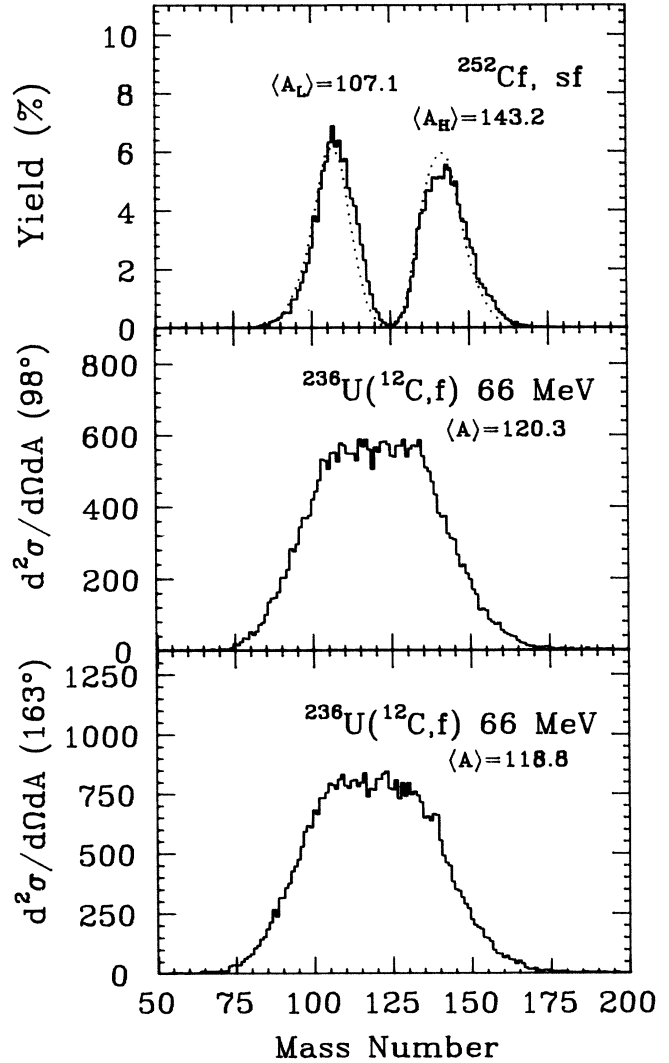


FIG. 5. Top: Mass yield curve for the ^{252}Cf spontaneous fission source (solid curve). The dotted curve shows the mass yield curve taken from the literature (Ref. 20). Middle: Double differential cross section (arbitrary units) for symmetric fragmentation in the reaction $^{236}\text{U}(^{12}\text{C},f)$ at 98° in the center-of-mass system. Bottom: The same as in the middle part, but for 163° in the center-of-mass system.

the expected value 119.5. If one considers the sign of the deviation of the Cf calibration spectrum from the literature curve, the first moment at 163° is slightly low, but we consider this deviation to be within the uncertainty of the calibration.

E. Elastic scattering angular distributions

In the course of these measurements we have also obtained some rudimentary elastic scattering distributions. For the ^{232}Th and ^{236}U targets the experimental resolution was insufficient to resolve inelastic excitations of the target. Our interest in these distributions has been to provide an estimate of the total reaction cross section, and to pro-

vide some constraints on the optical potential used in some theoretical approaches to understanding fusion. The angular distributions, shown in Fig. 6, are rather featureless, as expected for these heavy systems. They have been fitted using conventional optical potentials ($V \sim 30$ MeV, $W \sim 40$ MeV, $r_0 = 1.25$ fm, $a = 0.5$ fm). The total reaction cross sections obtained with these potentials are compared with the fission cross sections in Fig. 7. The general trend of an increasing fraction of the total reaction cross section to go into nonfusion channels as the bombarding energy is decreased is consistent with the observations of Videbaek *et al.*¹⁴ and Vulgaris *et al.*¹⁵ for the $^{16}\text{O} + ^{208}\text{Pb}$ system and of Rehm *et al.*²² for heavier projectiles.

IV. ANALYSIS

In this section we will compare our results with various theoretical models. In general, our approach will be to do this with as little parameter fitting as possible, making use of known properties whenever possible. We will start with the analysis of the excitation functions, as it is rather meaningless to try to understand the width of the spin distributions without the constraint of reproducing the observed total fusion cross section.

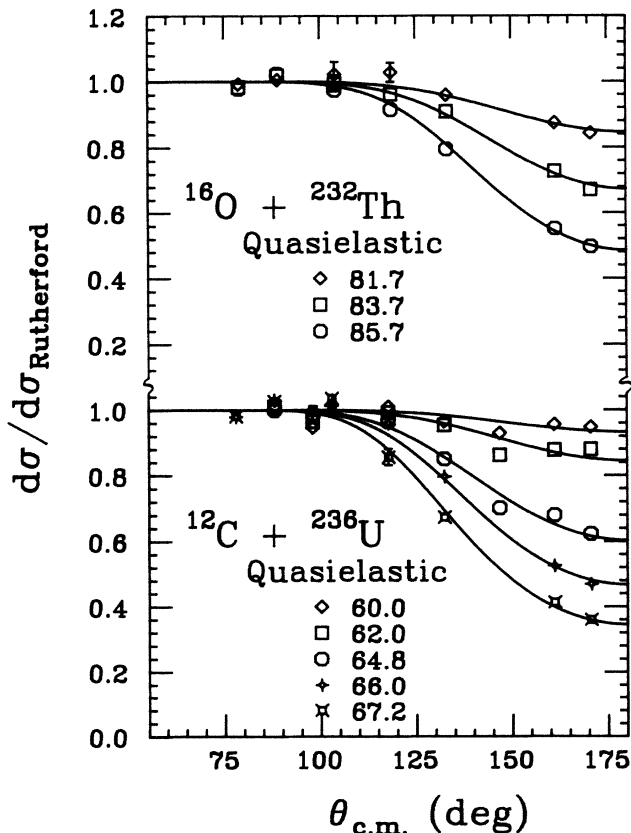


FIG. 6. Ratio of elastic to Rutherford cross sections for $^{12}\text{C} + ^{236}\text{U}$ and $^{16}\text{O} + ^{232}\text{Th}$ at several bombarding energies. The solid curves are optical model fits.

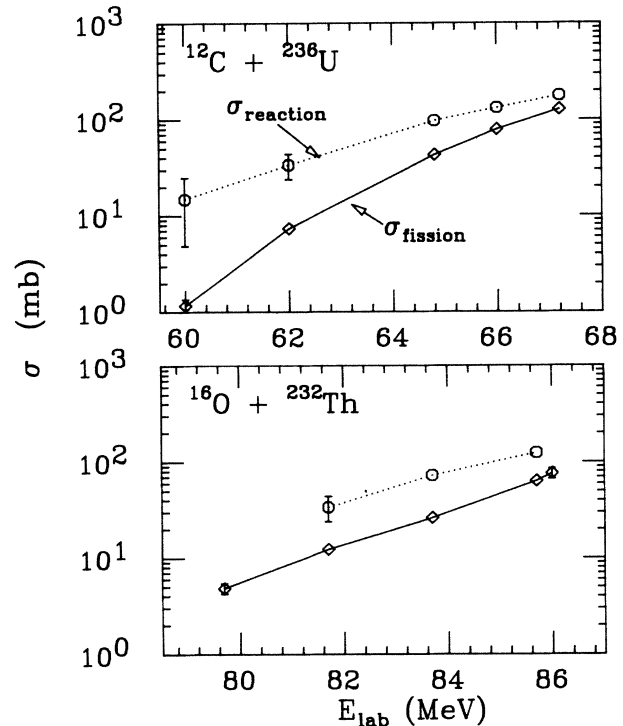


FIG. 7. Comparison of optical model total reaction cross sections with fusion excitation functions.

A. Cross sections

1. The Esbensen zero-point motion model

This model is actually more general than indicated by the title used, as it incorporates both the effect of static deformations and of zero-point motions of slow collective surface vibrations.²³ In the case of ^{208}Pb only vibrations about an equilibrium spherical shape are relevant, whereas for ^{232}Th and ^{236}U the static quadrupole deformations play a dominant role. The basic assumption of the model is that the shape of the nucleus is frozen during the course of the collision. This is a good approximation for rotational motion, and for low-lying collective vibrations. For high-lying vibrations, the collective modes will only influence the relative motion in an average manner, and their effect can be absorbed into the effective potential. This question has been addressed quantitatively by Esbensen *et al.*²⁴ For phonon energies large compared to 1 MeV, the vibrational enhancements are increasingly damped out. For this reason we have neglected the contributions of the projectile vibrations ($E = 4.43$ and 6.1 MeV in ^{12}C and ^{16}O , respectively). In the Esbensen model the shape fluctuations or the average over orientation for static deformations gives rise to a distribution in radii whose standard deviation is given by

$$\sigma_{\lambda} = \frac{R}{Z(\lambda+3)} \left[(2\lambda+1) \frac{B(E\lambda)}{B_W(E\lambda)} \right]^{1/2}$$

for vibrations and

$$\sigma_2 = R\beta_2 / (4\pi)^{1/2}$$

for permanent deformations. The relevant parameters for our target nuclei have been taken from various compilations²⁵ and are collected in Table II. Esbensen used a generalized nuclear potential based on the potential deduced from elastic scattering by Christensen and Winther.²⁶ The only parameter adjusted by Esbensen was a radius shift parameter ΔR . We adjust this parameter to fit the knee

of the excitation function, the region most sensitive to the barrier height determined by ΔR . The excitation functions obtained are shown in Fig. 8, and the values of ΔR used to obtain the fits are given in Table II. These values are close to the 0.29 value corresponding to the Christensen-Winther potential, and vary in the range Esbensen found necessary to fit Sm excitation functions. The ^{208}Pb cross sections are somewhat overpredicted. This is to be expected, as the energies and hence the vibra-

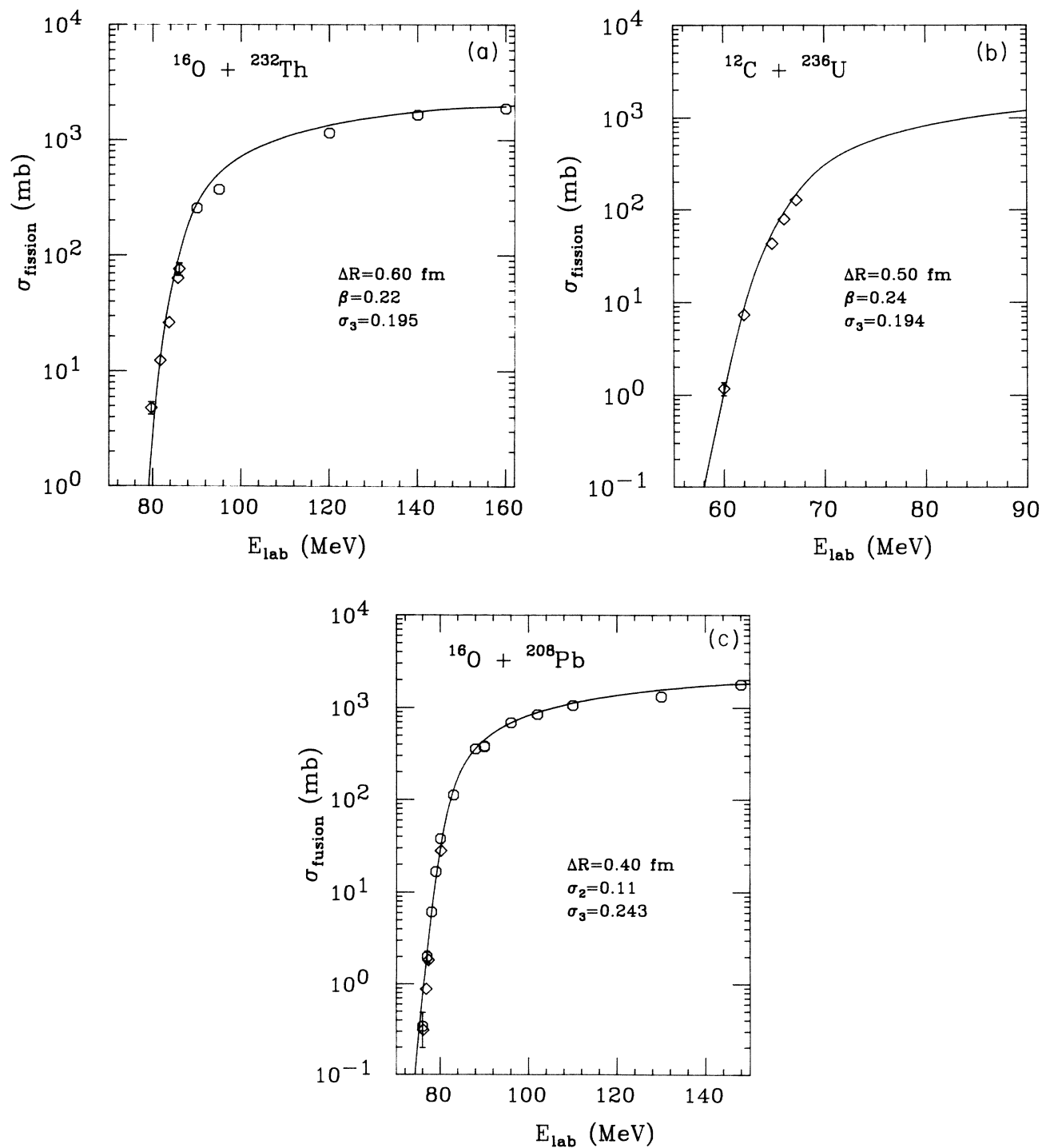


FIG. 8. Comparison of excitation functions with Esbensen model calculations.

tional frequencies of the 2^+ and 3^- states of ^{208}Pb are too high for the frozen-shapes approximation to be valid.²⁴ The $^{16}\text{O} + ^{232}\text{Th}$ excitation function is slightly under-predicted at the lowest energies. The reason for this is not clear, but may reflect the importance of transfer channels.

2. The Wong model

Although employing more approximations than the Esbensen model, this model²⁷ has the essential ingredients to reproduce the effects expected in permanently deformed nuclei. The barriers are represented by inverted parabolas and the penetration is calculated with the simple, closed-form Hill-Wheeler²⁸ expression. The barrier height is calculated as a function of orientation, and the appropriate average over orientations is performed. We have fixed the barrier curvature parameter $\hbar\omega$ at 4.0 to correspond to the barrier curvature obtained with realistic nuclear potentials.²⁹ Fits to the $^{12}\text{C} + ^{238}\text{U}$ excitation function indicate a preference for a smaller value ($\hbar\omega = 2.8$), a result also obtained in an earlier study⁷ of $^{12}\text{C} + ^{154}\text{Sm}$. We have used literature values of the quadrupole deformation as given in Table II, adjusting only the (spherical) barrier height. The striking success of this model in reproducing the differences in the slopes of the excitation functions at low energies is illustrated in Fig. 9, where we have plotted the cross sections as a function of energy relative to the barrier. We conclude from this comparison and the comparison with the Esbensen model that we have a reasonably good *a priori* understanding of the magnitude of the sub-barrier fusion cross section enhancements.

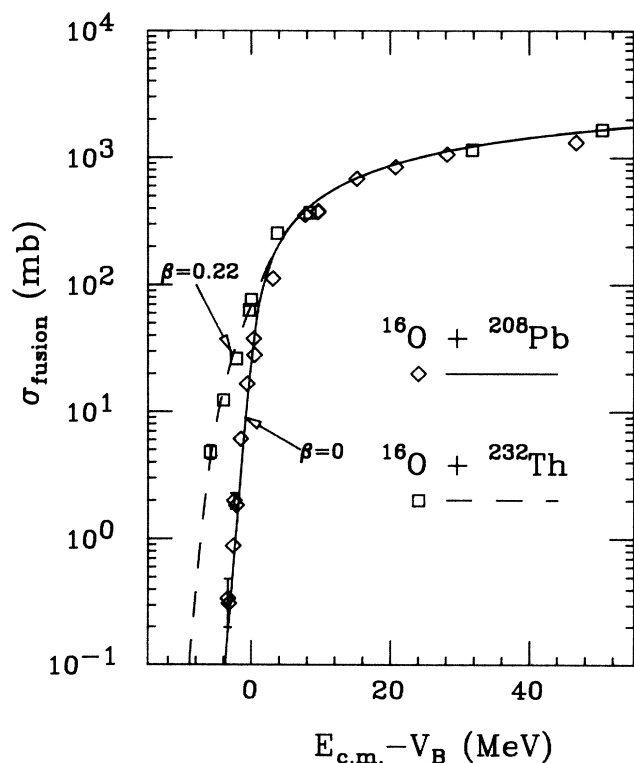


FIG. 9. Comparison of $^{16}\text{O} + ^{208}\text{Pb}$ and $^{16}\text{O} + ^{232}\text{Th}$ excitation functions with Wong model calculations, illustrating the dependence of the low-energy slopes on the target deformation.

3. Coupled-channels calculations

The coupled-channels approach can, in principle, give the most complete description of the reaction dynamics. The coupling of both inelastic and transfer channels to the elastic channel can be incorporated without making a frozen-shapes approximation. Most coupled channels calculations have only incorporated a few inelastic channels, and an imaginary potential is used to represent the absorption into both the unincorporated direct channels and the fusion channel. Two unusually complete coupled channels calculations have been performed for the $^{16}\text{O} + ^{208}\text{Pb}$ system by Thompson *et al.*³⁰ and by Pieper *et al.*³¹ These calculations included both transfer and inelastic channels, with the strength of the coupling to the transfer channels being made consistent with experimental observations.^{14,15} Since all of the important nonfusion channels are included explicitly, no imaginary potential in the surface region is necessary and the fusion cross section can be obtained either by using a short range imaginary potential or by applying an incoming-wave boundary condition. The real nuclear potential in the two calculations differ somewhat, but, in general, give a reasonable reproduction of the experimental elastic and fusion cross sections. The calculation of Thompson *et al.* has full recoil and exact finite-range couplings. Results have been reported for 80 and 102 MeV, where they reproduce the fusion cross section quite well. The calculations of Pieper *et al.* and of Thompson *et al.* give very similar spin distributions at 80 MeV. The comparison of the Pieper *et al.* calculations with the fusion cross sections is shown in Fig. 10, and with the transfer cross sections in their original paper.³¹ The calculations do quite well in accounting for the data, although a consistent tendency to overpredict both the transfer and fusion cross sections is apparent at the lowest energies.

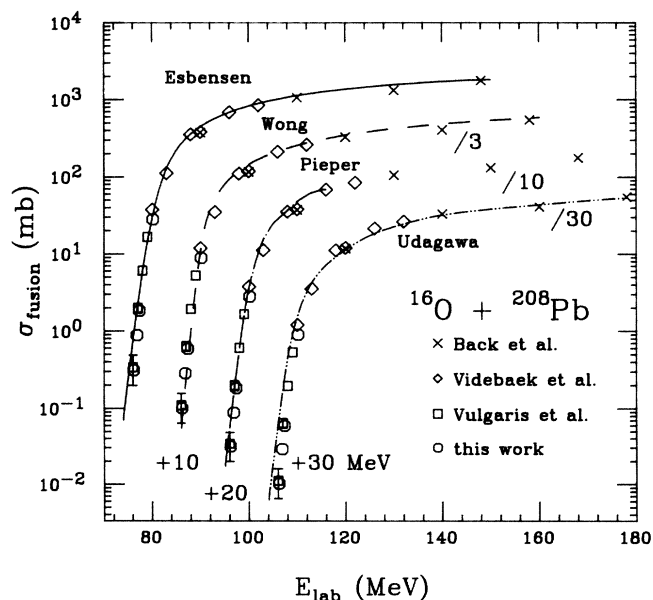


FIG. 10. Comparison of $^{16}\text{O} + ^{208}\text{Pb}$ excitation functions with several models.

4. Optical potential approaches

Recently, Udagawa, Kim, and Tamura³² (UKT) proposed a new fusion model based upon an optical potential which reproduces elastic scattering data. They dissected the imaginary part of the optical potential, $W(r)$, into two parts. One of them, $W_F(r)$, is responsible for the fusion reaction and the other, $W_{DF}(r)$, correlates to the direct reaction. Extending the usual relation between the total reaction cross section and $W(r)$, one can calculate the fusion cross section from

$$\sigma_F(E) = (\pi/k^2) \sum_{l=0}^{\infty} (2l+1) T_{F;l},$$

where the penetration factor for fusion, $T_{F;l}$, can be written as

$$T_{F;l} = (8/\hbar v) \int_0^{\infty} |\chi_l(r)|^2 W_F(r) dr.$$

Here, χ_l is the scattering wave function calculated with the full optical potential and v is the relative velocity. For simplicity, UKT set

$$W_F(r) = \begin{cases} W(r) & \text{for } r < R_F, \\ 0 & \text{for } r > R_F, \end{cases}$$

with

$$R_F = r_F (A_p^{1/3} + A_t^{1/3}).$$

Using a value $r_F = 1.45$ fm together with the known optical potential parameters from Ref. 14, UKT demonstrated that this model can explain the $^{16}\text{O} + ^{208}\text{Pb}$ fusion data in the incident energy range of 80–102 MeV. Following their success, we calculated fusion cross sections for the $^{16}\text{O} + ^{208}\text{Pb}$ system using the same r_F value at much

higher and lower energies. For the higher energies we used the optical potentials obtained by Ball *et al.*,³⁵ and for the lower energies we applied a Woods-Saxon potential which fits the new experimental elastic data at $E(^{16}\text{O}) = 78$ MeV.³⁴ These potentials are collected in Table III.

From Fig. 10 it is clear that the UKT model overestimates the absolute fusion cross section below $E(^{16}\text{O}) = 80$ MeV, though it accounts for the high energy data fairly well. Since our main interest is the spin distribution below the Coulomb barrier, we decided to reduce the r_F value to 1.40 fm for further comparisons with the spin distributions in order to avoid an enhancement of the mean spin value coming from the overestimation of the cross section. Reducing r_F from 1.45 to 1.40 fm reduces the fusion cross section from 50.5 to 31.5 mb, a value comparable to or less than given by the other models. It should be noted that this modification can improve fitting around $E(^{16}\text{O}) = 80$ MeV, but that below 78 MeV we still see a large (up to a factor of 5) discrepancy between the experimental fusion cross section and the model calculation. Moreover, the model calculation with $r_f = 1.40$ fm greatly underpredicts cross sections for high incident energies.

The penetration factors for fusion, $T_{F;l}$, obtained by the UKT model with $r_f = 1.40$ fm, are shown in Fig. 11 together with those from some of the other model calculations, parameters of which have been adjusted to reproduce the absolute cross section at $E = 80$ MeV. It is interesting to see that the UKT model predicts a slightly wider spin distribution than the other models. This might be simply because the UKT model allows fusion to occur during passage through the barrier, rather than requiring that barrier penetration be complete as in most models.

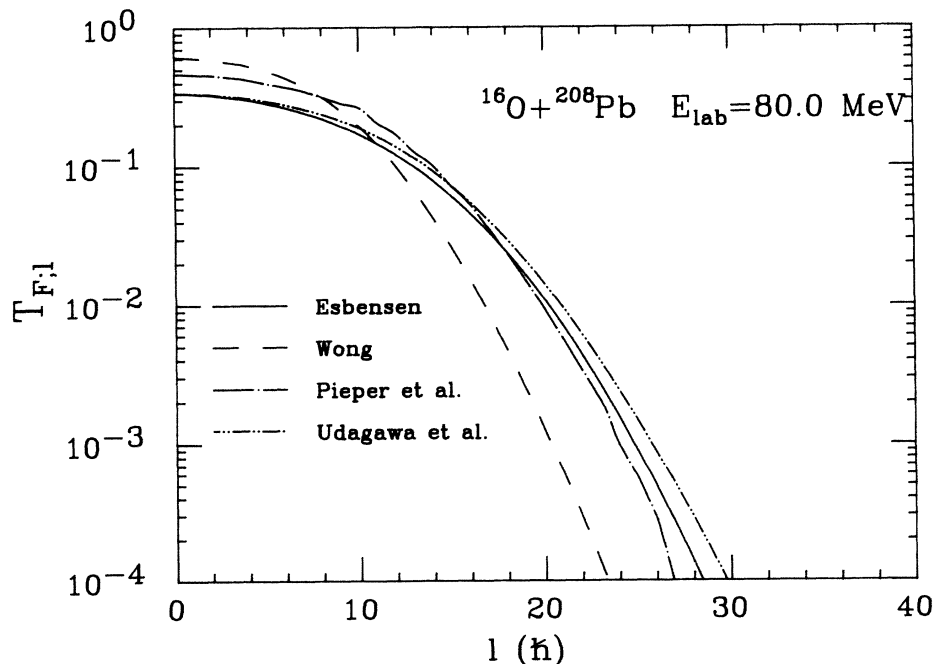


FIG. 11. T_l distributions for 80 MeV $^{16}\text{O} + ^{208}\text{Pb}$ as given by several models.

TABLE III. Optical potential parameters for $^{18}\text{O} + ^{208}\text{Pb}$.

E_{lab} (MeV)	V (MeV)	W (MeV)	r_0	a
≤ 78	100	10.78	1.246	0.5275
80	100	21.8	1.249	0.5
83	100	37.9	1.244	0.5
88	100	64.6	1.232	0.5
90	100	66.9	1.233	0.5
94	100	81.8	1.232	0.5
96	100	66.5	1.234	0.5
102	100	71.4	1.227	0.5
≥ 129.5	40	25	1.285	0.545

Thus, the UKT model naturally includes slightly larger impact-parameter processes, i.e., larger angular momentum processes. Consequently, the UKT model predicts the largest mean square spin value for the fusion reaction as can be seen in Fig. 12. However, the observed spin values are even larger than the UKT model predictions.

In the case of well-deformed nuclei like ^{232}Th and ^{236}U it is not so easy to apply the UKT model, because quite a large amount of fusion can take place through inelastic channels. To solve this problem one has to treat the inelastic channels by means of the coupled channels method and then calculate the absorption from those channels, too. Partly because of the complexity coming from the coupled channels calculation and partly because of the failure in the $^{16}\text{O} + ^{208}\text{Pb}$ system, we have not tried to apply the UKT model to the $^{16}\text{O} + ^{232}\text{Th}$ and $^{12}\text{C} + ^{236}\text{U}$ systems.

Nagarajan and Satchler³⁵ have also considered the spin distribution for the $^{16}\text{O} + ^{208}\text{Pb}$ reaction from a one-dimensional barrier penetration model. They particularly emphasize the energy dependence of the optical potential at near-barrier energies, as deduced from elastic scattering results³⁴ and expected from a dispersion relation.³⁶ They obtain a spin distribution at 80 MeV similar to the coupled-channels results of Thompson *et al.* and of Pieper *et al.* discussed below. As will be seen, this latter distribution underestimates the mean-square spin value deduced from the anisotropy.

B. Angular distributions

The angular distributions of fission fragments have been calculated using a statistical model^{37,38} for the relative probability of emitting fragments at different angles from an initial state of spin I . This probability is characterized by a parameter $K_0^2 = \mathcal{I}_{\text{eff}} T / \hbar^2$. In a transition-state model the effective moment of inertia is defined by $1/\mathcal{I}_{\text{eff}} = 1/\mathcal{I}_{\parallel} - 1/\mathcal{I}_{\perp}$, where \mathcal{I}_{\parallel} and \mathcal{I}_{\perp} are the saddle point shape moments of inertia about the nuclear symmetry axis and an axis perpendicular to this axis, respectively. For the reactions leading to the compound nucleus ^{248}Cf our calibration approach is more general and does

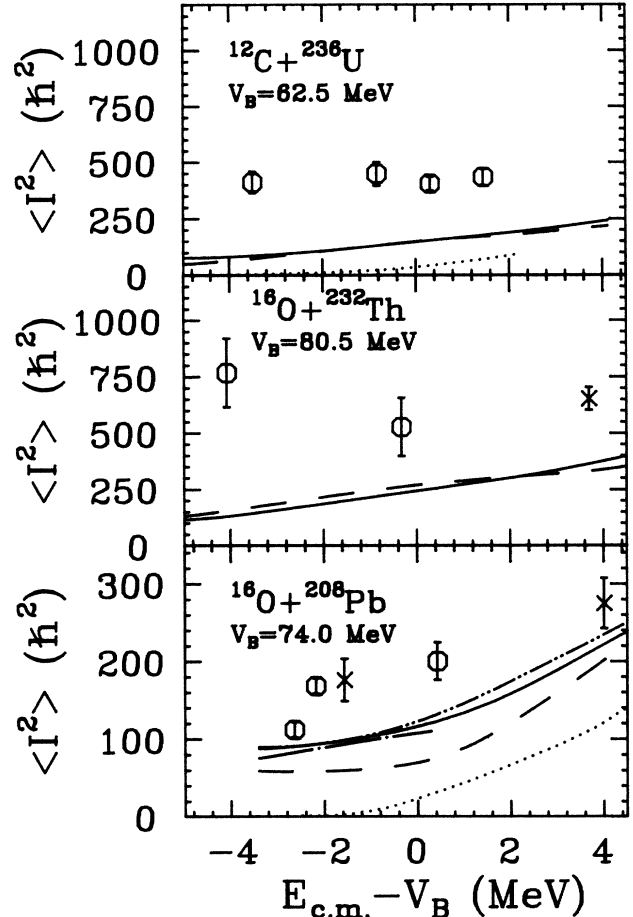


FIG. 12. Comparison of mean square spin values deduced from fission fragment anisotropies with different models. The dotted curves are based on the observed total fusion cross section together with the sharp cutoff approximation. The definitions of the other curves are the same as Fig. 11. The data represented by crosses in the figures are obtained from Back *et al.* (Ref. 17) and Vulgaris *et al.* (Ref. 15).

not require the assumption that the angular distributions are determined at the saddle point. We deduce K_0^2 for ^{248}Cf from the above-barrier $\alpha + ^{244}\text{Cm}$ anisotropy³⁹ and a calculated spin distribution. Since in this case the bombarding energy is nearly twice the barrier energy, the spin distribution is not very sensitive to model assumptions. A Wong model calculation or an optical model calculation, with a 7% correction for fission following inelastic processes, give similar values for $\langle I^2 \rangle$ of about $230\hbar^2$. From this value we deduce a K_0^2 parameter of 192 at a compound nuclear excitation energy of 36 MeV. This leads to an $\mathcal{I}_0/\mathcal{I}_{\text{eff}}$ ratio of 0.77, using a level density parameter of $a = A/8$. This can be compared to the value of 0.62 given by the diffuse surface liquid drop model of Sierk.⁴⁰ In the case of $^{16}\text{O} + ^{208}\text{Pb}$, no light-ion calibration data are available for the compound nucleus ^{224}Th . We have used the diffuse surface model⁴⁰ prediction of $\mathcal{I}_0/\mathcal{I}_{\text{eff}} = 1.0$. This value is in good agreement with the systematic dependence of $\mathcal{I}_0/\mathcal{I}_{\text{eff}}$ with Z^2/A .³⁸ The K_0^2

value is that obtained from the excitation energy above the barrier. A small correction for the dependence of $\mathcal{J}_0/\mathcal{J}_{\text{eff}}$ on spin is also included.

We have used these K_0^2 values, together with the spin distribution taken from the previously described fusion model calculations which reproduce the excitation functions, to calculate angular distributions. Comparisons of these calculations with experiment for the $^{12}\text{C}+^{236}\text{U}$ and $^{16}\text{O}+^{232}\text{Th}$ systems were shown in Ref. 11, and for the $^{16}\text{O}+^{208}\text{Pb}$ system are shown in Fig. 1. Irrespective of the model used, the anisotropy is qualitatively underestimated. This appears to be a uniquely sub- or near-barrier phenomenon. At higher energies (e.g., 120 MeV) our procedure successfully reproduces the anisotropy measured by Back *et al.*¹⁷ for $^{16}\text{O}+^{232}\text{Th}$.

In order to illustrate the discrepancy with the theoretical models discussed and to facilitate comparison with possible new models, we show in Fig. 12 the $\langle I^2 \rangle$ values deduced from the experimental anisotropies. The error bars include both the statistical error in the angular distribution and the systematic error from the uncertainty in the K_0^2 value obtained from the $\alpha+^{244}\text{Cm}$ reaction. Sample calculations indicate that corrections for spin distributions having different functional forms than the assumed distributions would be less than 10% and in a direction to increase the discrepancy with theoretical expectations. Also shown are mean square spin values calculated from various models. The deduced mean-square spin values are several times larger than expected, and except for the $^{16}\text{O}+^{208}\text{Pb}$ system appear to have saturated at a high value at the lowest energy studied.

V. DISCUSSION

We have measured fission cross sections and angular distributions to considerably lower energies than previously investigated. The excitation functions are well behaved, exhibiting the features expected on the basis of the nuclear structure of the target nuclei. The angular distributions are much more anisotropic than expected. Assuming compound nucleus formation, the angular distributions imply larger mean-square spin values than expected. We first consider the possibility that a compound nucleus is not formed prior to fission, compromising the deduction of spin values from the anisotropy. The magnitude of the fission barrier relative to the nuclear temperature is discussed in the context of a previous suggestion about a necessary condition for achieving statistical equilibrium at the saddle point. We also review other information on spin distributions to see if there are any kinds of discrepancies between experiment and expectations.

A. Is quasifission responsible for large anisotropies?

Quasifission is usually defined as fission following capture behind the entrance-channel (conditional or frozen-mass-asymmetry) barrier, but without formation of a compound nucleus with a shape more compact than that of the unconditional saddlepoint. That is, it is fission corresponding to evolution along the mass-asymmetry degree of freedom at deformations larger than that of the saddle point. Such fission will lead to more anisotropic fragment

distributions, either because the angular momentum bearing degrees of freedom are never relaxed, or because K equilibration takes place at a shape more extended than that of the unconditional saddle. Thus a sizeable contribution of quasifission could perhaps account for our observations. It has been pointed out that in the case of a quasifission reaction the mass-differential angular distribution is not necessarily symmetric with respect to 90° , and may exhibit an enhancement of projectile-like fragments at forward angles.⁴¹⁻⁴³ Integration over all masses would, of course, result in an angular distribution symmetric with respect to 90° , since quasifission is a binary reaction.

A systematic study of quasifission has been reported by Toke *et al.*⁴² In a study of near-barrier fission of various targets with 6 MeV/nucleon ^{238}U , they find no evidence for quasifission with ^{16}O and clear evidence with ^{48}Ca . From their Fig. 9 it appears to us that the mass-angle contour plots for ^{27}Al are consistent with only a modest contribution of a quasifission distribution of the kind exhibited by ^{48}Ca . Toke *et al.*,⁴¹ however, have concluded from the surprisingly large anisotropy of the fission fragment angular distribution $^{27}\text{Al}(^{238}\text{U},f)$ that a major part of the cross section (70%) should be referred to as quasifission. In this reaction a considerable dependence of the first moment of the mass distribution on angle can be observed, indicating an enhancement of the cross section for projectile-like fragments at forward angles. This is in contrast to the $^{16}\text{O}(^{238}\text{U},f)$ reaction, where the cross section was interpreted as "true" compound nucleus fission, and the first moment of the mass distribution is independent of the angle. We have found no evidence for a dependence of the mass distribution on angle, and the shapes of the distributions are as expected for complete-fusion fission. The yield of fragments intermediate in mass between that of the projectile and that of typical light fission fragments was negligible. We conclude that, although there is no proof for "true" compound nucleus fission, there is at least no indication that a significant part of the observed cross section is related to quasifission. Thus it seems unlikely that we would see a significant contribution with ^{16}O and especially with ^{12}C induced fission.

B. Are the fission barriers too low to expect equilibration at the saddle point?

It has been proposed^{44,45} that larger-than-expected anisotropies in high energy heavy reactions may result if the angular momentum dependent fission barrier $[B_f(l)]$ drops below the nuclear temperature T . For such partial waves statistical equilibrium may not be established at the saddle point, and larger than expected anisotropies can arise either because K equilibration is only achieved at a later stage or because the K distribution is determined by the entrance channel dynamics. We have examined this possibility for our system, and find that for our low excitation energies (and hence low temperatures) and modest angular momenta a negligible fraction of the compound nuclei have fission barriers smaller than the temperature. This is illustrated in Fig. 13, where the l distributions

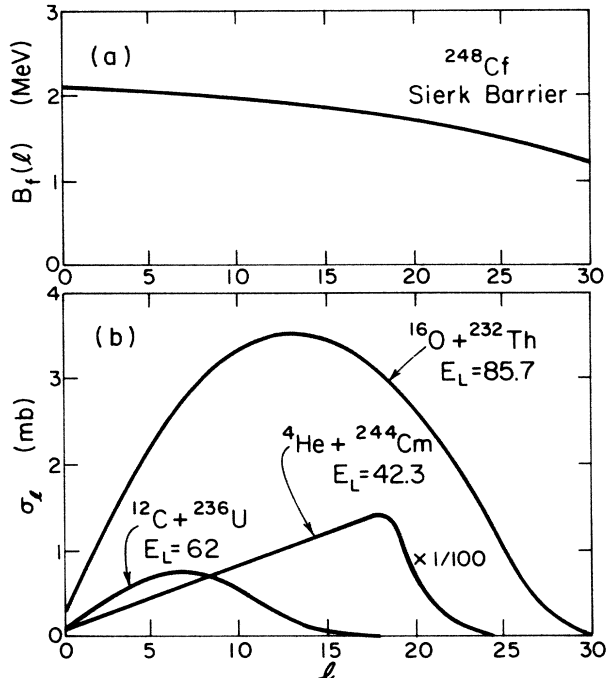


FIG. 13. Spin distributions for several systems are compared. Also shown is the spin dependence of the fission barrier as calculated by Sierk, showing that few partial waves lead to nuclei with fission barriers smaller than the nuclear temperature of about 1 MeV.

given by the Wong model for several systems, including the $\alpha + {}^{244}\text{Cm}$ calibration reaction, are illustrated. Also shown is the l dependence of the fission barrier as given by Sierk's diffuse surface rotating droplet model.⁴⁰ The nuclear temperature in all of these systems is close to 1 MeV, so very few compound nuclei satisfy the criterion that $B_f(l) < T$. This figure also shows that the expected spin distributions for the systems we have studied are rather comparable to that of the calibration reaction, further strengthening the validity of our conclusion.

C. Possible role of Coulomb excitation in perturbing spin distributions

It has occurred to us and to others¹⁰ that Coulomb excitation might suppress fusion for the lower partial waves. The ${}^{232}\text{Th}$ and ${}^{236}\text{U}$ have low-lying states with large $B(E2)$'s which can be strongly Coulomb excited, especially for the lowest partial waves. Coulomb excitation takes energy from the kinetic energy of relative motion and puts it into the internal excitation energy of the target. The reduction in the relative kinetic energy would make the fusion reaction more sub-barrier and could lower the fusion probability. We have made some exploratory investigations of the likely magnitude of this effect both by looking at the results of a semiclassical calculation⁴⁶ and by running some coupled channels calculations.⁴⁷ We conclude that the perturbation of the spin distribution due to Coulomb excitation is small compared to the magni-

tude of the discrepancies that we observe. Also, our study of the ${}^{16}\text{O} + {}^{208}\text{Pb}$ system was motivated in part by the desire to study a system where Coulomb excitation effects would be small.

D. Relationship to earlier work

We have concluded from this study that the spin distributions in sub-barrier fusion are broader than current theoretical estimates. One might ask whether there are indications of this in other work. Indeed, looking back at some of the earlier work, there are hints of this discrepancy at somewhat higher bombarding energies. In several studies^{42,17} of fission fragment anisotropies the $\mathcal{J}_0/\mathcal{J}_{\text{eff}}$ values at the lowest energy show a sudden increase, although often the statistical uncertainties of the underlying anisotropies were large. An anomalously large value of $\mathcal{J}_0/\mathcal{J}_{\text{eff}}$ will be extracted if the mean-square spin assumed is too small. The most comprehensive previous study at near-barrier energies is that of Back *et al.*¹⁷ They used deformation values more than twice as large as the known values. The use of such unphysically large deformations means that the spin distributions are much broader than expected. For the lighter system ${}^{16}\text{O} + {}^{208}\text{Pb}$, Pieper *et al.*³¹ have already remarked that their calculation gives overly small anisotropies when compared with the data of Videbaek *et al.*¹⁴

With regard to information about spin distribution widths from other types of experiments, we have only a few γ ray multiplicity studies to consider. Earlier work^{6,7} on ${}^{12}\text{C}$ and ${}^{16}\text{O}$ induced fusion with ${}^{154}\text{Sm}$ did not show any anomaly, but was limited to near-barrier energies. Nolan *et al.*⁹ have recently reported multiplicity distributions for ${}^{80}\text{Se} + {}^{80}\text{Se}$. Dasso *et al.*¹⁰ have been able to reproduce the general features of these distributions, but in so doing have overestimated the relative fusion cross section by factors of 2–3 at the lowest energies. This discrepancy suggests that it might be difficult to reproduce the distributions with the constraint of reproducing the excitation function.

VI. CONCLUDING REMARKS

We have found that fission anisotropies at sub-barrier energies are much larger than expected. Assuming compound nucleus formation, we obtain spin distributions with larger mean-square values than expected. The fragment-fragment folding angle correlations, the shape of the mass distributions and their independence on angle, and the persistence of the discrepancy to effective fissionabilities way below the empirical threshold for quasi-fission, all support a compound nuclear interpretation. It is possible that the underestimation of the anisotropies in the ${}^{12}\text{C} + {}^{236}\text{U}$ and ${}^{16}\text{O} + {}^{232}\text{Th}$ systems may arise from the neglect of transfer channels⁴⁸ in the models employed. The calculations of Pieper *et al.* for the ${}^{16}\text{O} + {}^{208}\text{Pb}$ system, however, include the effect of transfer channels and the discrepancy between experiment and calculation persists. We are therefore led to the conclusion that we still have an inadequate understanding of all of the dynamical features of subbarrier fusion in heavy systems.

There is one assumption in essentially all sub-barrier

fusion models presently employed that may be questionable. This is the assumption that the effective mass appearing in the quantum mechanical barrier penetration expression is the reduced mass of the system. This may be a reasonable assumption for light systems or for not overly high energies where the inner classical turning point occurs at internuclear separations corresponding to small density overlaps. For heavier systems at sub-barrier energies, the overlap may become more appreciable. Little is known about the dependence of the inertial mass on internuclear separation, although a few time-dependent Hartree-Fock calculations have been performed for light systems.^{49,50} These calculations show significant increases in the effective mass at separations less than the top of the interaction barrier for $l=0$ collisions. The dependence of the increase on l is unknown, but one could speculate that if it were smaller for higher l 's than for lower l 's, then the use of the reduced mass rather than the true inertial mass might lead to higher mean-square spin values.

Note added in proof. We have recently become aware of an observation that calls into question our assumption that sequential fission (fission following transfer) is negligible compared to fusion followed by fission for the $^{16}\text{O}+^{232}\text{Th}$ reaction. Leigh *et al.* [J. R. Leigh, R. M. Diamond, A. Johnston, J. O. Newton, and S. H. Sie, *Phys. Rev. Lett.* **42**, 153 (1979)] have measured the yield of fission fragments in coincidence with projectile-like fragments emitted to very backward angles. If we assume an angular distribution of the $\cos^2\theta$ form back of 90° , as is typical for sub-barrier transfer angular distributions, we estimate from the data of Leigh *et al.* that there is approximately 10% sequential contamination of our fission

yield at 86 MeV and 30% at 80 MeV. Since the anisotropy in coincidence with transfer products is not known, it is difficult to assess how important a correction to the mean square spin values will result from this contamination, but it may be significant. Sequential fission is less likely to be as important for the $^{12}\text{C}+^{236}\text{U}$ reaction as the optimum Q value for two-proton transfer corresponds to a smaller residual excitation energy. This is consistent with our observations of smaller discrepancies compared to expectations for the latter system. Some contamination must be expected, however, as Cheifitz *et al.* [E. Cheifitz, H. C. Britt, and J. B. Wilhelmy, *Phys. Rev. C* **24**, 519 (1981)] were able to see fission fragments in coincidence with breakup alphas from the $^{236}\text{U}(^{12}\text{C}, ^8\text{Be})$ reaction. Fission following transfer should not be a problem in the $^{16}\text{O}+^{208}\text{Pb}$ reaction since the fission barrier is twice as high as for the heavier targets and no transfers are expected to lead to large enough excitation energies for sequential fission to occur.

ACKNOWLEDGMENTS

We thank Gorm Nykreim for performing some of the model calculations. We are indebted to S. Steadman and W. Henning for providing us with unpublished data, and to A. Sierk for making his finite-range fission barrier and saddle point moment-of-inertia code available to us. We thank B. B. Back, S. Bjørnholm, I. Halpern, S. Landowne, and S. Pieper for helpful discussions. We thank D. Cline for performing a sample Coulomb excitation calculation for us. This work was supported in part by the U. S. Department of Energy.

*Also at: Department of Chemistry, University of Washington, Seattle, WA 98195.

†Present address: Lockheed Palo Alto Research Laboratory, Palo Alto, CA 94304.

¹B. Sikora *et al.*, *Phys. Rev. C* **20**, 2219 (1979).

²R. G. Stokstad, Y. Eisen, S. Kaplanis, D. Pelte, U. Smilansky, and I. Tserruya, *Phys. Rev. C* **21**, 2427 (1980).

³M. Beckerman *et al.*, *Phys. Rev. Lett.* **45**, 1472 (1980); *Phys. Rev. C* **23**, 1581 (1981).

⁴R. Vandenbosch, in *Heavy Ion Fusion Reactions*, Proceedings of the Tsukuba International Symposium, Sept. 1984, edited by K. Furuno and T. Kishimoto (World-Scientific, Singapore, 1985).

⁵W. Reisdorf *et al.*, *Phys. Rev. Lett.* **49**, 1811 (1982).

⁶R. Vandenbosch *et al.*, *Phys. Rev. C* **28**, 1161 (1983).

⁷S. Gil *et al.*, *Phys. Rev. C* **31**, 1752 (1985).

⁸B. Haas *et al.*, *Phys. Rev. Lett.* **54**, 398 (1985).

⁹P. J. Nolan *et al.*, *Phys. Rev. Lett.* **54**, 2211 (1985).

¹⁰C. H. Dasso, J. D. Garrett, and S. Landowne, *Phys. Lett.* **161B**, 36 (1985).

¹¹R. Vandenbosch, T. Murakami, C.-C. Sahm, D. D. Leach, A. Ray, and M. J. Murphy, *Phys. Rev. Lett.* **56**, 1234 (1986).

¹²S. B. Kaufman, E. P. Steinberg, B. D. Wilkins, J. Unik, A. J. Gorski, M. J. Fluss, *Nucl. Instrum. Methods* **115**, 47 (1974).

¹³V. E. Viola, K. Kwiatkowski, and M. Walker, *Phys. Rev. C*

31, 1550 (1985).

¹⁴F. Videbaek, R. B. Goldstein, L. Grodzins, and S. G. Steadman, *Phys. Rev. C* **15**, 954 (1977).

¹⁵E. Vulgaris, L. Grodzins, R. Ledoux, and S. Steadman, *Phys. Rev. C* **33**, 2017 (1986).

¹⁶V. E. Viola, Jr. *et al.*, *Phys. Rev. C* **26**, 178 (1982).

¹⁷B. B. Back *et al.*, *Phys. Rev. C* **32**, 195 (1985); **33**, 385 (1986).

¹⁸K. Hartel, Ph.D. thesis, Technical University of Munich, 1985.

¹⁹A. Gavron, *Phys. Rev. C* **21**, 230 (1980).

²⁰K. F. Flynn *et al.*, *Phys. Rev. C* **6**, 2211 (1972).

²¹A. H. Wapstra and G. Audi, *Nucl. Phys.* **A432**, 1 (1985).

²²K. E. Rehm *et al.*, *Phys. Rev. Lett.* **55**, 280 (1985).

²³H. Esbensen, *Nucl. Phys.* **A352**, 147 (1981).

²⁴H. Esbensen, Jian-qun Wu, and G. F. Bertsch, *Nucl. Phys.* **A411**, 275 (1983).

²⁵M. B. Lewis, *Nucl. Data Sheets B* **5**, 243 (1981); W. T. Milner, C. E. Bemis, Jr., and F. K. McGowan, *Phys. Rev. C* **16**, 1686 (1977); M. R. Schmorak, *Nucl. Data Sheets* **36**, 867 (1982).

²⁶P. R. Christensen and A. Winther, *Phys. Lett.* **65B**, 19 (1976).

²⁷C.-Y. Wong, *Phys. Rev. Lett.* **31**, 766 (1973).

²⁸D. L. Hill and J. A. Wheeler, *Phys. Rev.* **89**, 1102 (1953).

²⁹U. Jahnke, H. H. Rossner, D. Hilscher, and E. Holub, *Phys. Rev. Lett.* **48**, 17 (1982).

³⁰I. J. Thompson, M. A. Nagarajan, J. S. Lilley, and B. R. Ful-

- ton, Phys. Lett. **157B**, 250 (1985).
- ³¹S. C. Pieper, M. J. Rhoades-Brown, and S. Landowne, Phys. Lett. **162B**, 43 (1985).
- ³²T. Udagawa, B. T. Kim, and T. Tamura, Phys. Rev. C **32**, 124 (1985); B. T. Kim, T. Udagawa, and T. Tamura, *ibid.* **33**, 370 (1986).
- ³³J. B. Ball, C. B. Fulmer, E. E. Gross, M. L. Halbert, D. C. Hensley, C. A. Ludemann, M. J. Saltmarsh, and G. R. Satchler, Nucl. Phys. **A252**, 208 (1975).
- ³⁴J. S. Lilley, B. R. Fulton, M. A. Nagarajan, I. J. Thompson, and D. W. Banes, Phys. Lett. **151B**, 181 (1985).
- ³⁵M. A. Nagarajan and G. R. Satchler, Phys. Lett. **173B**, 29 (1986).
- ³⁶M. A. Nagarajan, C. Mahaux, and G. R. Satchler, Phys. Rev. Lett. **54**, 1136 (1985); C. Mahaux, H. Ngo, and G. R. Satchler, Nucl. Phys. **A449**, 354 (1986).
- ³⁷I. Halpern and V. M. Strutinsky, in *Proceedings of the U.N. and International Conference on Peaceful Uses of Atomic Energy* (United Nations, New York, 1958), Vol. 15, pp. 408 and 1513.
- ³⁸R. Vandenbosch and J. R. Huizenga, *Nuclear Fission* (Academic, New York, 1973).
- ³⁹R. F. Reising, G. L. Bate, and J. R. Huizenga, Phys. Rev. **141**, 1161 (1966).
- ⁴⁰A. Sierk, Phys. Rev. C **33**, 2039 (1986).
- ⁴¹J. Toke, R. Bock, Dai Guang-xi, A. Gobbi, S. Gralla, K. D. Hildenbrand, J. Kuzminski, W. F. J. Müller, A. Olmi, W. Reisdorf, S. Bjørnholm, and B. B. Back, Phys. Lett. **142B**, 258 (1984).
- ⁴²J. Toke *et al.*, Nucl. Phys. **A440**, 327 (1985).
- ⁴³K. Lützenkirchen, J. V. Kratz, G. Wirth, W. Brüche, L. Dörr, K. Sümmerer, R. Lucas, J. Poitou, C. Gregoire, and S. Bjørnholm, Z. Phys. A **320**, 529 (1985).
- ⁴⁴A. Gavron *et al.*, Phys. Rev. Lett. **52**, 589 (1984).
- ⁴⁵V. S. Ramanurthy and S. S. Kapoor, Phys. Rev. Lett. **54**, 178 (1985); Phys. Rev. C **32**, 2182 (1985).
- ⁴⁶A. Winther and J. deBoer, in *Coulomb Excitation*, edited by K. Alder and A. Winther (Academic, New York, 1966).
- ⁴⁷Computer code ECIS79, written by J. Raynal, was used for these calculations.
- ⁴⁸R. A. Broglia, C. H. Dasso, S. Landowne, and A. Winther, Phys. Rev. C **27**, 2433 (1983).
- ⁴⁹H. Flocard, P. H. Heenan, and D. Vautherin, Nucl. Phys. **A339**, 336 (1980).
- ⁵⁰P. H. Heenen, H. Flocard, and D. Vautherin, Nucl. Phys. **A394**, 525 (1983).